

2011

In Vitro Models for Glaucoma Research: Effects of Hydrostatic Pressure

Yuan Lei
Imperial College London

Shadi Rajabi
University of Toronto


Ryan M. Pedrigi
University of Nebraska-Lincoln, rpedrigi@unl.edu

Darryl R. Overby
Imperial College London

A. Thomas Read
University of Toronto

See next page for additional authors

Follow this and additional works at: <http://digitalcommons.unl.edu/mechengfacpub>

 Part of the [Mechanics of Materials Commons](#), [Nanoscience and Nanotechnology Commons](#), [Other Engineering Science and Materials Commons](#), and the [Other Mechanical Engineering Commons](#)

Lei, Yuan; Rajabi, Shadi; Pedrigi, Ryan M.; Overby, Darryl R.; Read, A. Thomas; and Ethier, C. Ross, "In Vitro Models for Glaucoma Research: Effects of Hydrostatic Pressure" (2011). *Mechanical & Materials Engineering Faculty Publications*. 298.
<http://digitalcommons.unl.edu/mechengfacpub/298>

This Article is brought to you for free and open access by the Mechanical & Materials Engineering, Department of at DigitalCommons@University of Nebraska - Lincoln. It has been accepted for inclusion in Mechanical & Materials Engineering Faculty Publications by an authorized administrator of DigitalCommons@University of Nebraska - Lincoln.

Authors

Yuan Lei, Shadi Rajabi, Ryan M. Pedrigi, Darryl R. Overby, A. Thomas Read, and C. Ross Ethier

In Vitro Models for Glaucoma Research: Effects of Hydrostatic Pressure

Yuan Lei,^{1,2,3} Shadi Rajabi,^{2,4,5} Ryan M. Pedrigi,¹ Darryl R. Overby,¹ A. Thomas Read,⁴ and C. Ross Ethier^{1,4,5,6}

PURPOSE. The response of cells (e.g., optic nerve head [ONH] cells) to mechanical stress is important in glaucoma. Studies have reported the biological effects of hydrostatic pressure on ONH cells cultured on a rigid substrate. An apparatus, designed to independently vary hydrostatic pressure and gas tension (including oxygen tension) in culture medium, was used to evaluate the effects of pressure and tension on cell migration, shape, and α -tubulin architecture in a transformed cell line (DITNC1 rat cortical astrocytes).

METHODS. During the assay period, cells were exposed to one of four experimental configurations: (1) control pressure and control gas tension; (2) high-pressure (7.4 mm Hg) and reduced gas tension; (3) control pressure and reduced gas tension; and (4) high-pressure and control gas tension.

RESULTS. Calculations suggested that the cells in configurations 2 and 3 were hypoxic, as confirmed by direct measurements in configuration 2. No effects of hydrostatic pressure were observed on cell migration or α -tubulin architecture. However, cells cultured under low gas tension (configurations 2 and 3) showed increased migration at 48 and 72 hours ($P < 0.05$).

CONCLUSIONS. A hydrostatic pressure of 7.4 mm Hg has no effect on DITNC1 astrocytes cultured on rigid coverslips, whereas hypoxia associated with a fluid column creating this pressure does. These results differ from those in a previous report, the results of which may be explained by altered gas tensions in the culture medium. Steps are recommended for control of secondary effects when testing the effect of pressure on cultured cells. (*Invest Ophthalmol Vis Sci.* 2011;52:6329–6339) DOI:10.1167/iov.11-7836

Elevated intraocular pressure (IOP) remains the primary risk factor for the development of glaucomatous optic neuropathy. Consistent, sustained, and significant reduction of IOP slows visual field loss,¹ and thus there is a great deal of interest

in understanding how the mechanical stimulus imposed by IOP affects the function of ocular cells, including trabecular meshwork cells,² retinal ganglion cells,³ and optic nerve head astrocytes.⁴ For example, research toward this end has used rodent^{3,5–8} or monkey models⁹ in which IOP was elevated, either spontaneously or by intervention.

Recently, studies have been published that have used an alternate model: the application of hydrostatic pressure to cells cultured on a rigid substrate.^{2–8,10–14} These studies have used optic nerve head astrocytes and retinal ganglion cells, among other ocular cell types, and have generally shown that the application of hydrostatic pressure leads to significant biological effects, such as increased apoptosis of retinal ganglion cells^{5,7} and alterations in astrocyte morphology,² migration,⁴ proliferation,⁴ cytoskeletal organization, elastin synthesis,¹⁰ and neural cell adhesion molecule (NCAM) production.¹¹ Because of its simplicity, the application of hydrostatic pressure to cultured cells appears very attractive for examining the effects of elevated IOP in glaucoma, and it has been advanced as a model system for this purpose.

However, there are reasons to believe that the application of hydrostatic pressure as described in those reports is not a good model system for studying the mechanobiological effects of elevated IOP. For example, depending on how the pressure is applied, this approach alters gas tensions (including oxygen tension) in the culture medium, raising the possibility that some of the biological effects reported in the papers were artifacts of low oxygen tension or other gas tension changes (e.g., changes in pH caused by changes in the level of carbon dioxide dissolved in the medium).

The first goal of the present work is to present the design of an experimental apparatus for separating the effect of hydrostatic pressure and gas tension on cultured cells (i.e., to permit application of hydrostatic pressure with no change in oxygen tension to cultured cells, or vice versa). The second goal was to use this apparatus to evaluate the cellular response to elevated hydrostatic pressure and/or gas tension, so as to help us understand whether previously reported effects were due to pressure alone, gas tensions alone, or both.

METHODS

Design of the Experimental Apparatus

In this study, cells were exposed to two levels of oxygen tension and two levels of hydrostatic pressure, for a total of four different experimental conditions. These were achieved by using the following experimental configurations (Fig. 1):

1. Normal pressure, normal gas tension in culture medium (control condition). Two experimental configurations were used to create these conditions. In configuration 1A, the cells were grown on coverslips placed at the bottom of vertical columns filled with 15 mm of medium, similar to the arrangements commonly used for cell culture. This was the same arrangement as that used by Salvador-Silva et al.⁴ In

From the ¹Department of Bioengineering, Imperial College London, London, United Kingdom; and the ⁴Department of Mechanical and Industrial Engineering, the ⁵Institute of Biomaterials and Biomedical Engineering, and the ⁶Department of Ophthalmology and Vision Sciences, University of Toronto, Toronto, Ontario, Canada.

²These authors contributed equally to the work presented here and should therefore be regarded as equivalent authors.

³Present affiliation: Research Centre, Eye and ENT Hospital, Fudan University, Shanghai, China.

Supported by the American Health Assistance Foundation (CRE) and a Royal Society Wolfson Research Excellence Award (CRE). SR was financially supported by NSERC.

Submitted for publication May 6, 2011; revised May 31, 2011; accepted May 31, 2011.

Disclosure: **Y. Lei**, None; **S. Rajabi**, None; **R.M. Pedrigi**, None; **D.R. Overby**, None; **A.T. Read**, None; **C.R. Ethier**, None

Corresponding author: C. Ross Ethier, Department of Bioengineering, Imperial College, South Kensington Campus, London SW7 2AZ, UK; r.ethier@imperial.ac.uk.

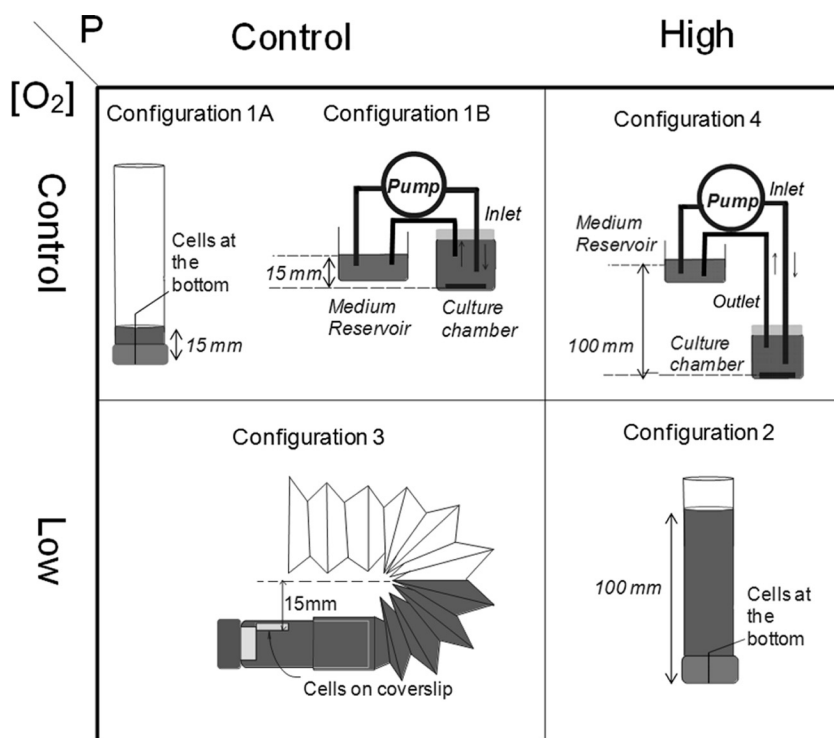


FIGURE 1. Four different experimental conditions created by the five sets of specially designed experimental apparatus. Configurations 1A and 1B for control condition; configuration 4 for elevated pressure and normal oxygen tension; configuration 3 for normal pressure and reduced oxygen tension; configuration 2 for elevated pressure and reduced oxygen tension. Each system is filled with medium so the free surface of medium is 15 mm (control pressure) or 100 mm (elevated hydrostatic pressure) above the level of the cells on the coverslips; P, pressure; $[O_2]$, oxygen concentration.

configuration 1B, the cells were placed in a closed culture chamber, and a peristaltic pump (multichannel PD5001; Heidolph Brinkmann, Saffron Walden, UK) was used to circulate medium between a reservoir exposed to incubator gases and the culture chamber. This arrangement supplied fresh medium in equilibrium with the incubator gases to the cells inside the culture chamber and was used as a control for configuration 4. This design and that of configuration 4 were originally proposed by Obazawa et al.¹⁵

- Elevated pressure, reduced oxygen tension in medium. In configuration 2, cells on a coverslip were grown under a static column of medium producing a pressure of 7.4 mm Hg (liquid column height, 100 mm). This replicates the high pressure experiments of Salvador-Silva et al.⁴ As we show below, cultured cells are exposed to reduced oxygen tensions in this configuration.
- Normal pressure, reduced oxygen tension in medium. In configuration 3, cells were grown in contact with a horizontally oriented volume of medium. The system was designed in such a way to give the same reduced gas tensions as in configuration 2, but the same pressure on the cells as in configurations 1.
- Elevated pressure, normal oxygen tension in medium. Configuration 4 was the same as configuration 1B, except that the medium reservoir was placed at a height of 100 mm above the cells to produce the same pressure as in configuration 2 (7.4 mm Hg) but normal oxygen tension.

Vertical (configurations 1A and 2) and horizontal (configuration 3) columns were made by cutting off the round end of a glass culture tube (160 mL, with screw cap; VWR, Mississauga ON, Canada) to give a total tube length of 185 mm for vertical columns or 105 mm for horizontal columns. The corrugated part of the horizontal column was a segment of fluoroethylene polymer (FEP) tubing (length, 12 in.; inner diameter [ID], 1.5 in.; outer diameter [OD], 2 in.; minimum curvature radius, 2 in.; cuff length, 2 in.; Industrial Rubber Ltd., Mississauga, ON, Canada). A polycarbonate platform fit inside the cap end of each horizontal column, and the coverslip was mounted on the platform with a small amount of silicone vacuum grease (VWR) applied to the back of the coverslip. The cells in configuration 3 were oriented upside down with the coverslip adhering to the bottom of the polycarbonate platform

(Fig. 1), but this orientation is likely to be unimportant, since many adherent cells are oriented upside down *in vivo*, and the net gravitational force on a single cell (of order pN) is negligible with respect to cell-substrate adhesion forces. In configurations 1A and 3, medium was added so that the height of the free surface was 15 mm above the coverslip.

In the pump system (configurations 1B and 4), the cylindrical culture chamber was made by cutting off the top of a 30-mL beaker (Cole-Parmer Canada, Montreal, QC, Canada). The medium reservoir used in the pump systems was a 50-mL beaker (Cole-Parmer). The tubing that connected the culture chamber and the medium reservoir was chemically and biologically inert tubing (internal diameter, 0.25 mm; OD outer diameter, 2.08 mm; Pharmed; Cole-Parmer), selected in part because of its very low permeability to gases, including oxygen. The stopper used to seal the cell culture chamber was made of FDA-approved platinum-cured silicone (Cole-Parmer). The stoppers were custom drilled so that a piece of tubing (Pharmed; Cole-Parmer) and a polycarbonate tube could pass through while maintaining a gas-tight seal. The polycarbonate tube was attached to the outlet tube (polyethylene tubing, ID, 1.14 mm; Cole-Parmer; Fig. 1). The medium was pumped from the medium reservoir to the culture chamber via the inlet tubing (Pharmed; Cole-Parmer) and was then recirculated to the medium reservoir via the outlet polycarbonate tube.

Calculations Underlying Design of Apparatus

As part of our experimental design, we estimated the oxygen levels that cells would be exposed to in the configurations described above. This required knowledge of the initial oxygen tension in bottles of cell culture medium, since the vacuum filtration used by the manufacturer to sterilize the medium could affect dissolved gas tensions. We therefore measured the oxygen tension in culture medium at room temperature, using a fiber optic oxygen sensor (OxyMicro system with MicroTip; WPI UK, Stevenage, UK), calibrated by a two-point calibration (0% and 100% air saturation), according to the manufacturer's recommendations. Immediately after opening a previously unopened bottle of culture medium, we placed the oxygen sensor in the medium with the tip positioned along the centerline approximately halfway down

the bottle and took an oxygen concentration reading. This process was repeated in three different bottles of medium.

For modeling purposes, we assumed that the diffusivity of oxygen in the culture medium at 37°C was $3 \times 10^{-9} \text{ m}^2/\text{s}$ ¹⁶ and that oxygen solubility in culture medium was 1.01 mM/atm, this latter value differing slightly from the solubility of oxygen in water at 37°C (1.06 mmol/L/atm) due to the composition of culture medium.¹⁷ We further assumed that the composition of gas in the incubator was a mixture of 95% dry air and 5% CO₂ at 100% relative humidity. The partial pressure of oxygen in dry air is 0.2095 atm, but the high CO₂ and H₂O vapor levels in the incubator gas reduce the oxygen partial pressure in the incubator atmosphere to 0.187 atm.¹⁷ This implies that the concentration of oxygen in medium in equilibrium with the incubator gas at 37°C and 1 atm is 0.188 mM. In a study by Rouleau et al.,¹⁸ the oxygen consumption rate of a rat spinal cord glial cell line was reported to be 12.1 fmol/min/cell in early cultures, which translates into 2.02×10^{-16} moles O₂/s/cell. This number, although it is measured for a general rat glial cell line, is very close to that calculated using the studies by Jacobson et al.¹⁹ and Hasselblatt et al.²⁰ with rat cortical astrocytes. Jacobson et al.¹⁹ measured the oxygen consumption rate for these cells to be 35.1 nanomoles oxygen/min/mg of protein. Hasselblatt et al.²⁰ stated that the average protein content of wild-type rat cortex astrocytes was 20 μg for 60,000 astrocytes. From these data, the oxygen consumption rate by a single astrocyte from rat cortex is calculated to be 1.95×10^{-16} moles O₂/s/cell. Consistent with all these data, we assumed an oxygen consumption rate of $\beta = 2 \times 10^{-16}$ moles O₂/s/cell for the DITNC1 astrocytes used in this study.

Vertical Columns: Configurations 1A and 2. The distribution of oxygen in the stagnant normal and high hydrostatic pressure vertical columns (Fig. 1) was estimated using calculations and numerical simulations. Oxygen was assumed to be transported only by diffusion, so that the governing equation for the local concentration, c , is simply

$$\frac{\partial c}{\partial t} = D\nabla^2 c \quad (1)$$

where D is the diffusivity of oxygen in culture medium. The initial oxygen concentration in the medium was assumed to be uniform and equal to c_o , and the medium at the top surface was assumed to be in equilibrium with incubator gases, leading to a fixed oxygen concentration c_{top} at the top surface:

$$c(z = L) = c_{top} \quad (2)$$

$$c(t = 0) = c_o \quad (3)$$

where z is the vertical direction normal to the cells, $z = 0$ is the cell surface and $z = L$ is the free surface of the fluid column.

Finally, at the level of the cells, we assumed that the diffusional flux of oxygen supplied the consumption of oxygen by the cells (i.e., that the oxygen concentration obeys)

$$D \frac{\partial c}{\partial z} \Big|_{z=0} = \frac{\beta n}{\pi r^2} \quad (4)$$

where β is the oxygen consumption rate per cell, n is the number of cells on the coverslip, and r is the radius of the coverslip on which the cells reside.

For long-duration experiments, the steady state solution of equation 1 subject to equations 2 and 4 is of interest. Steady oxygen transport was computed by finite element modeling using commercial software (Fluent, ver. 6.2.16; Fluent Inc., Lebanon, NH). Briefly, since the vertical column is rotationally symmetric, a 2-D finite element mesh was generated on a vertical plane comprising half the cross-sectional area of the column (Gambit, ver. 2.2.30, Fluent Inc.). The tube walls were assumed to be impermeable to oxygen, and the number of cells

on the coverslip was assumed to be 30,000.¹⁷ This is the number of cells initially seeded onto the coverslip and is therefore a conservative estimate that neglects cell proliferation.

Although the above steady calculation is a useful starting point, we must also consider unsteady effects, which arise from two sources: the increase in oxygen consumption as the cells on the coverslip proliferate, and the depletion of the oxygen in the medium over time as cells consume oxygen in the medium. To account for the former effect, we assume that the number of cells, n , increases according to

$$n = n_o e^{\gamma t} \quad (5)$$

where γ is a suitable rate constant for cell growth, t is time and n_o is the number of cells originally seeded onto the coverslip. The above growth model assumes continuous exponential growth, which will break down as the cells approach confluence, particularly if the cells are contact inhibited.

If we assume a constant oxygen consumption rate per cell, then equation 4 becomes

$$D \frac{\partial c}{\partial z} \Big|_{z=0} = \frac{\beta n_o}{\pi r^2} e^{\gamma t} \quad (4a)$$

A quasi-steady one-dimensional solution of equation 1 subject to equations 2 and 4a exists for the special case in which the equilibration time for the oxygen concentration in the fluid column is much faster than the characteristic cell division time, in which case the unsteady term in equation 1 can be neglected. Assuming that the diffusion can be treated as one-dimensional, which is reasonable, since the coverslip covers most of the base of the fluid column and the cells are seeded uniformly onto the coverslip, then the quasi-steady oxygen concentration in the culture medium at the level of the cells is given by

$$c(z = 0, t) = c_{top} - \frac{L n_o \beta e^{\gamma t}}{\pi r^2 D} \quad (6)$$

The inherently unsteady case is more complex, and there is no exact solution to equation 1 subject to equations 2, 3, and 4a that we are aware of. However, a useful approximate solution to equation 1 can be found by noting the form of the solution: there will be an oxygen deficit adjacent to the cells that will propagate into the medium (away from the cells). Over a time τ the characteristic propagation distance of this deficit is $\sqrt{2D\tau}$, which for oxygen over a 3-day duration (the longest interval between medium changes) gives a propagation distance of 39 mm, which is less than the 100-mm fluid column height for configuration 2. Thus, to a first approximation, the medium column in configuration 2 (although not in configuration 1A) can be treated as semi-infinite. If we further assume that the diffusion is one-dimensional in the z -direction, we can then seek a solution to

$$\frac{\partial c}{\partial t} = D \frac{\partial^2 c}{\partial z^2} \quad (1a)$$

subject to equations 3 and 4a.

This problem has been considered by Chaudhry and Zubair,²¹ who present the solution as

$$c(z, t) = c_o - \frac{n_o \beta e^{\gamma t}}{2\pi r^2 \sqrt{\gamma D}} [e^{-2\sqrt{\gamma z^2/4D} \operatorname{erfc}(\sqrt{z^2/4Dt} - \sqrt{\gamma t})} - e^{-2\sqrt{\gamma z^2/4D} \operatorname{erfc}(\sqrt{z^2/4Dt} + \sqrt{\gamma t})}]$$

where erfc is the complementary error function. This can be evaluated at the level of the cells ($z = 0$) and simplified to obtain

$$c(z = 0, t) = c_o - \frac{n_o \beta e^{\gamma t}}{\pi r^2 \sqrt{\gamma D}} \operatorname{erf}(\sqrt{\gamma t}) \quad (7)$$

where erf is the error function. Equation 7 was evaluated numerically.

Horizontal Columns: Configuration 3. According to the same logic as for configuration 2, gas tensions experienced by cells in configuration 3 will be determined by the propagation of an oxygen deficit away from the cells, which will approximately follow equation 7 with z now referring to horizontal distance from the cells. Therefore, so long as the length of the medium column is ~ 100 mm and the maximum elapsed time between medium changes is 3 days or less, the oxygen tensions experienced by cells in configuration 3 are predicted to be the same as for configuration 2. Thus, in principle, any arrangement that exposes cells on the coverslip to the same pressure as in the control configuration (configuration 1A; Fig. 1) with a medium column of ~ 100 -mm length is acceptable for configuration 3. However, it is foreseeable that one might wish in future experiments to consider longer elapsed time between medium changes or other combinations of parameters that lead to oxygen transport being quasi-steady in configuration 3. We therefore also carried out steady simulations of oxygen diffusion (Fluent software; Fluent), with the goal of having an oxygen concentration on the coverslip equal to that for the vertical high hydrostatic column (configuration 2; Fig. 1) under steady conditions.

Pump System: Configurations 1B and 4. Suitable dimensions of the culture chamber, the positions of the inlet and outlet tubes, and the medium flow rate were determined by simulations of fluid flow and oxygen transport, with the goal of exposing the cells to the minimum possible shear stress from flowing medium (to avoid the effects of mechanostimulation) while providing them with adequate oxygen. We considered the oxygenation to be adequate if all cells on the coverslip experienced an oxygen tension $\geq 95\%$ of the oxygen tension in the medium in the inlet tubing.

To carry out the simulations, the distance between the outlet and the inlet and how deep the tubes would be inserted into the flask were chosen. The simulations were then begun, using an initial value for the inlet fluid speed, and the maximum of the computed shear stress on the surface of the coverslip (which was located at the bottom of the culture flask) was compared to a threshold value of 1×10^{-3} Pa, which is several orders of magnitude smaller than the smallest values of shear stress reported in the literature to have appreciable effects on cells.²²⁻²⁴ If the value of shear stress on the surface of the coverslip was smaller (or larger) than the threshold value, the inlet speed was accordingly increased (or decreased), and the simulations were repeated until the maximum shear stress on the surface of the coverslip was within a few percentage points of 10^{-3} Pa. The oxygen concentration distribution over the cross-section of the culture chamber was then obtained from this final simulation. This process was repeated with different tube locations and lengths, until a combination was found with low shear stress and adequate oxygenation.

Cell Culture Experiments

DITNC1 cells, a transformed cell line obtained from brain diencephalon tissue of 1-day-old rats, were purchased from ATCC (CRL-2005; London, UK). These cells show phenotypic characteristics of a type 1 astrocyte cell line.²⁵ The cells were cultured according to the supplier's recommendations in ATCC-formulated Dulbecco's modified Eagle's medium (ATCC UK) containing 10% fetal bovine serum (Sigma-Aldrich, Poole, UK). The cells were grown in T75 flasks (Corning Life Sciences, Chorges, France) in an incubator at 37°C with a fully humidified mixture of 95% air and 5% CO₂. They were subcultured before confluence with 1× trypsin EDTA solution (Sigma-Aldrich) when necessary.

We characterized the growth rate of DITNC1 cells by plating 150,000 cells on each of several 35 mm dishes (BD Biosciences, UK). Cultures were collected in suspension at various time points following plating using 1× trypsin EDTA solution, and the cells were counted with a hemocytometer.

After previous reports,⁴ we examined the effects of hydrostatic pressure and oxygen tension on DITNC1 cells using a cell migration assay and α -tubulin staining, as described below.

Experimental Creation of a Cell-Free Area and Migration Assay. We used a cell migration assay to study the effects of hydrostatic pressure. In this assay, a cell-free area (CFA) was created within a confluent monolayer of cells, and cell migration into the CFA was measured. Cells were seeded onto 22-mm diameter circular cover slips (VWR) at a density of 30,000 cells/coverslip, where the center of the coverslip was masked by a polydimethylsiloxane disc (PDMS, 4 mm diameter; Sylgard 184; Dow-Corning, Barry Wales, UK). The coverslips were then placed in plastic Petri dishes and cultured under standard conditions for 5 days, including a single change of culture medium on the third day. This produced a confluent or near-confluent layer of DITNC1 cells on the coverslip.

On the sixth day, the PDMS disc was carefully lifted using a pair of fine forceps to create a CFA. The CFA was then imaged (see below), the coverslips were carefully transferred into one of the experimental configurations shown in Figure 1 and a suitable amount of fresh medium was very gently added to create the relevant level of pressure. Cultures were left undisturbed in the incubator without change of medium for either 24, 48, and 72 hours, after which point they were removed and images of the CFA were taken using an inverted phase-contrast microscope (DM 1L; Leica, Wetzlar, Germany) and a digital camera (DF 360FX; Leica, Solms, Germany). Length measurements were calibrated using a hemocytometer slide incorporating a standardized grid. Data were expressed as the reduction in area (in square millimeters) of the CFA (i.e., the difference between the area of the CFA when it was formed and the area of the CFA at each later time point). The CFA data were analyzed by ANOVA with Bonferroni correction (SPSS 17; SPSS, Chicago, IL).

During culture experiments, the laboratory ambient pressure was routinely measured using a weather station (BAR908HG_UV; Oregon Scientific, Maidenhead, UK). Ambient pressures ranged from 750 to 762 mm Hg (0.987–1.003 atm), which was comparable to the imposed hydrostatic pressures. Therefore, all experiments were run in a parallel manner (i.e., coverslips were placed in high- and low-pressure configurations at the same time, and the CFAs were measured in each configuration at the same time so that high- and low-pressure cultures experienced the same variations in atmospheric pressure during each experiment. For purposes of computing oxygen concentrations in medium from percentage saturation values, we did not account for variations in ambient pressure, which will lead to a maximum error of less than 6% in oxygen tension.

α -Tubulin Staining. For α -tubulin immunostaining, DITNC1 cells from selected experiments above were fixed with 4% paraformaldehyde (PFA) for 10 minutes at room temperature at specific time

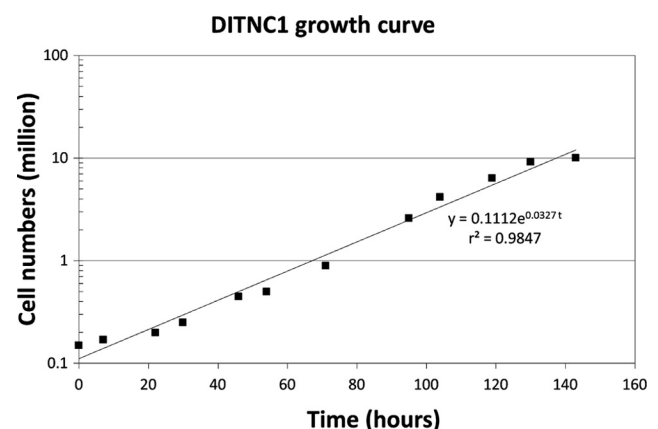


FIGURE 2. Growth curve for DITNC1 cells (log-linear plot), with fitted regression line shown superimposed on data. Each data point is the average of two determinations.

points (24, 48, or 72 hours after creation of the CFA). Fixed cells were rinsed in Dulbecco's phosphate-buffered saline (DPBS), permeabilized with 0.2% Triton X-100 in DPBS for 5 minutes at room temperature, washed again with DPBS and then blocked with 10% goat serum in DPBS for 30 minutes at room temperature. Cells were incubated with mouse monoclonal α -tubulin antibody (1:1000 in DPBS; Abcam, Cambridge, UK) for 30 minutes at room temperature, followed by three 5-minute washes in DPBS, and then an incubation with Alexa Fluor 546 goat anti-mouse IgG (1:200 in DPBS; Invitrogen, Paisley, UK) for 30 minutes at room temperature. Tubulin immunofluorescence was visualized with an epifluorescence microscope (Olympus, Tokyo, Japan; objective lens, DPlan 40 \times NA 0.65 160/0.17; Olympus).

Oxygen Measurements. Under experimental conditions identical with those described above for measurement of the CFA, direct oxygen tension measurements were made in cell culture medium for configurations 1A, 2, and 4 using a fiber-optic system (Neofox; Ocean Optics, Basildon, UK) with the fiber-optic probe mounted on a micro-manipulator (M3301R; WPI UK). Immediately after the coverslip was positioned in the appropriate configuration and placed in the incubator at the start of the experiment, the fiber-optic probe was inserted into the medium so that the probe tip was as close as possible to the cells (typically within 100 μ m). For configurations 1A and 4, no modifications to the apparatus were needed, while for configuration 2 a small hole was drilled in the lid of the culture chamber to allow the probe to pass while maintaining a seal. The probe remained in place throughout the experiment so as not to disturb the oxygen concentration profile within the medium, and oxygen readings were taken

either every 12 or 24 hours. It was not possible to suitably modify the apparatus to allow oxygen tension measurements to be made in configuration 3.

RESULTS

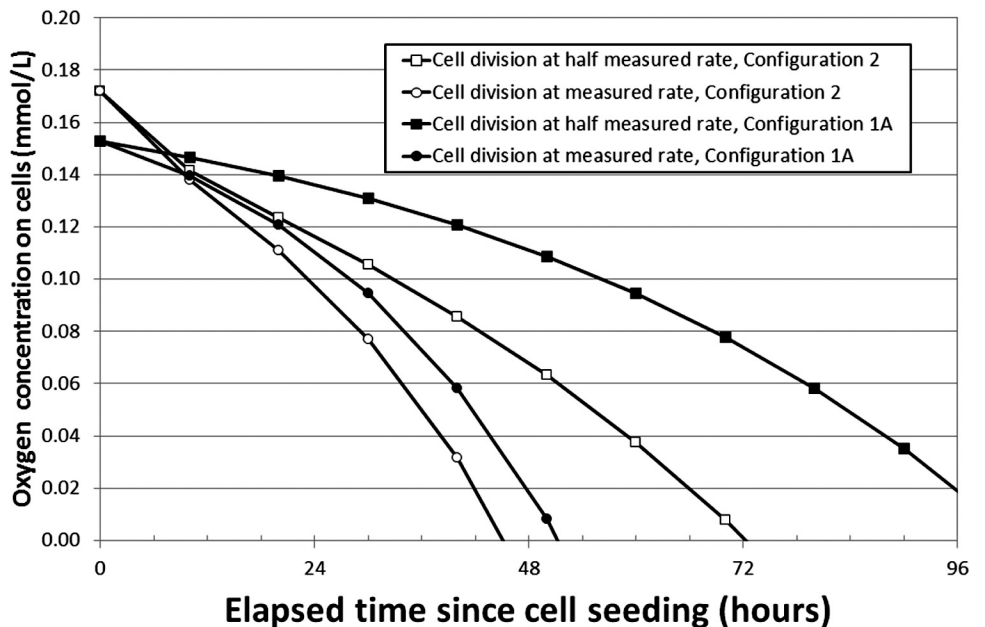
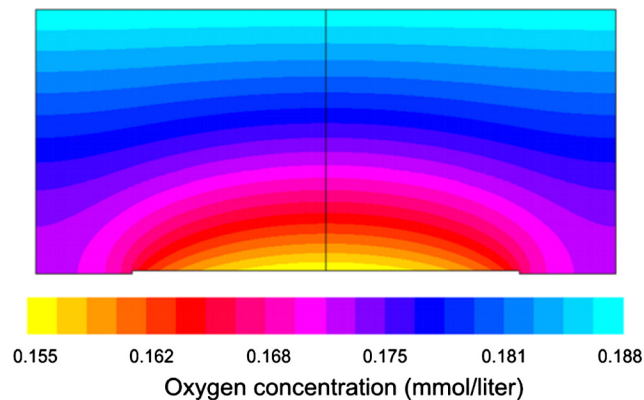
At room temperature, the oxygen concentration in newly opened bottles of culture medium was measured to be 17% \pm 0.5% (mean \pm SD; $n = 3$), slightly less than the oxygen concentration in room air (\sim 21%). We used the value of 17% as the initial oxygen concentration in the medium, c_o , for all subsequent calculations. Using the oxygen solubility coefficient for culture medium (see the Methods section), this is equivalent to a concentration of 0.172 mM.

The growth curve of DITNC1 cells is shown in Figure 2. Regression to this data showed that the rate constant for cell growth, γ , was 0.0327 hour $^{-1}$ (equation 5).

Design Calculations

Fluid Columns: Configurations 1A and 2. The characteristic time for attainment of a steady oxygen concentration profile in a fluid column of depth L subject to equations 2 and 4 is of order $L^2/4D$. For the control pressure vertical columns (configuration 1A), where the medium depth is $L = 15$ mm, this time is approximately 5 hours. This can be compared with the characteristic time for cell growth, $1/\gamma$, which is approximately 31

FIGURE 3. Computed oxygen concentrations at the cell surface under various conditions. *Top:* the computed concentration for configuration 1A under steady conditions for the situation in which there are 30,000 DITNC1 cells on the coverslip. *Bottom:* the computed concentration at the level of the cells in configurations 1A and 2 versus time, as obtained from analytical calculations (equations 6 and 7, respectively). The data shown are for an initial seeding of $n_o = 30,000$ cells. The plotted values for configuration 1A should be ignored near time 0, since equation 6 does not capture the initial transient equilibration as oxygen tensions approach the quasi-steady solution. For the same reason, equation 6 predicts that the oxygen concentration at time 0 is $c_{top} - (Ln_o\beta/\pi r^2 D)$ rather than c_o , which explains the offset of the two sets of curves at time 0. As discussed in the text, this initial transient lasts for several diffusional equilibration times, $L^2/4D$, which is approximately 5 hours for configuration 1A, after which the model predictions for configuration 1A become more valid. Note also that inclusion of this initial transient would cause the concentrations predicted for configuration 1A to be greater than those plotted.



hours. Thus, diffusion equilibrates at a rate nearly sixfold faster than cell growth, indicating that for configuration 1A, oxygen transport can be approximated as quasi-steady for much of the experiment, with a continuously increasing oxygen consumption rate at the bottom of the column (due to cell proliferation).

Since oxygen transport in configuration 1A is approximately quasi-steady, it is useful to first consider the idealized steady case. For a fixed population of 30,000 cells on the coverslip, computed contours of oxygen tension under steady conditions are shown in the Figure 3, top. This figure shows that the one-dimensional approximation for oxygen transport is reasonable (and is even more so for configuration 2 on account of its larger aspect ratio) and further indicates that the oxygen concentration at the level of the cells would be only slightly reduced compared with the oxygen tension at the free (top) surface of the medium. If we now account for cell division, the quasi-steady nature of the oxygen transport indicates that the oxygen concentration distribution will remain approximately linear, similar to the distribution shown in the Figure 3, top, except that the oxygen contour levels, including the oxygen tension experienced by the cells, will decrease over time as the cells proliferate. This is expressed by equation 6, which is plotted for some specific cases in Figure 3, bottom. If cells continue to divide at the rate shown in Figure 2, oxygen tensions at the level of the cells are predicted to approach 0 (assuming no change in consumption rate per cell) approximately 2 days after the initial seeding with 30,000 cells. In reality, there is likely to be a reduction in the metabolic rate of the cells, in their growth rate, or both as the local oxygen tensions decreased. For example, if growth rate, γ , decreased by a factor of two, then the cells would not experience hypoxic conditions until approximately 4 days after seeding.

The situation with the high pressure columns (configuration 2) is slightly different. The characteristic time for approaching a steady concentration profile in this configuration $L^2/(4D)$ is approximately 231 hours, and thus gas transport is inherently unsteady and the analytical formula given in equation 7 applies. If cells proliferate at the rate shown in Figure 2, equation 7 predicts that the oxygen tension at the level of the cells approaches zero after approximately 2 days (Fig. 3, bottom), similar to the situation in configuration 1A. However, unlike the situation for configuration 1A, a halving of cell division rate delays the onset of hypoxia by approximately 1 day in configuration 2, as opposed to a 2+ day delay for configuration 1A.

Pumped Systems: Configurations 1B and 4. The chosen dimensions for the culture flask in the pump design are given in Figure 4. This design provided cells with good oxygenation while exposing them to only very small shear stresses, with an average oxygen tension experienced by the cells over the entire coverslip predicted to be approximately 98% of the inlet value.

Horizontal Tube: Configuration 3. Computed oxygen tensions for the horizontal tube (Fig. 1) under steady conditions are illustrated in Figure 5. For the optimum length of the glass tube (66 mm), cells were predicted to experience oxygen tensions similar to those in high-pressure vertical columns (configuration 2). Note that although this result is for steady oxygen transfer, as discussed in the methods, a similar equivalence between oxygen tensions in configurations 3 and 2 is expected to hold for the unsteady case.

Experimental Measurements of Oxygen Tensions

In configuration 1A, measured oxygen concentrations at the level of the cells decreased over the first 24 hours until reach-

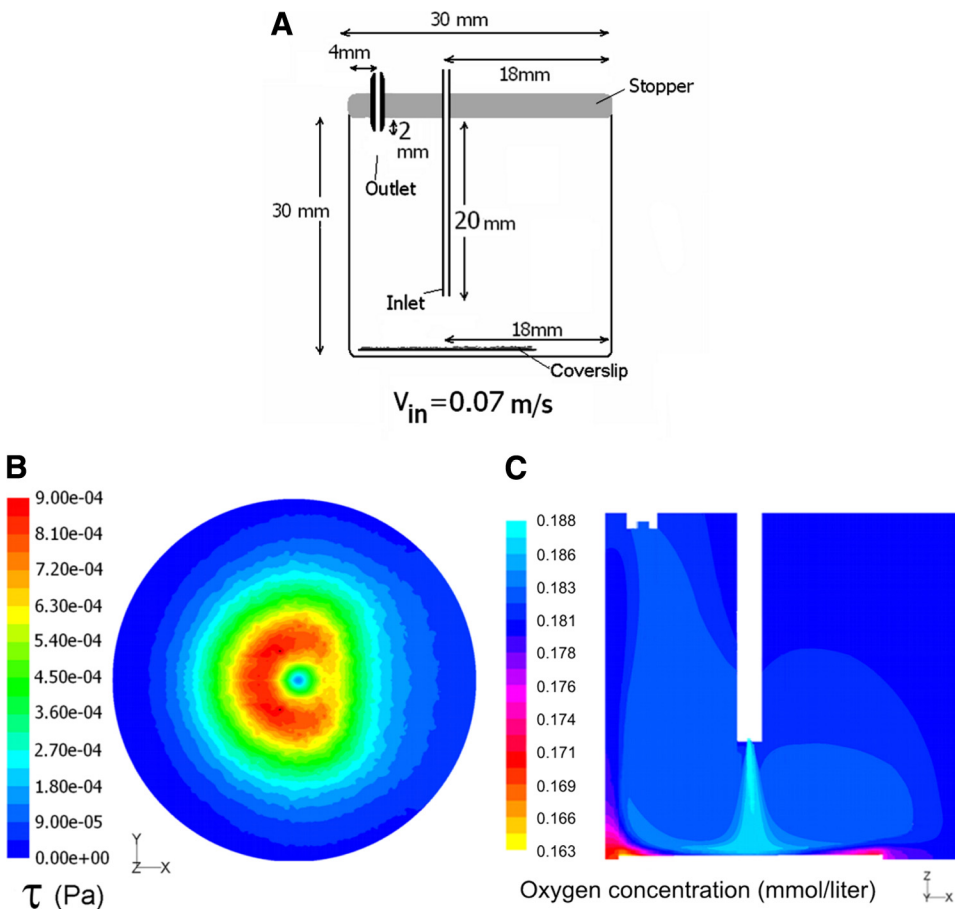
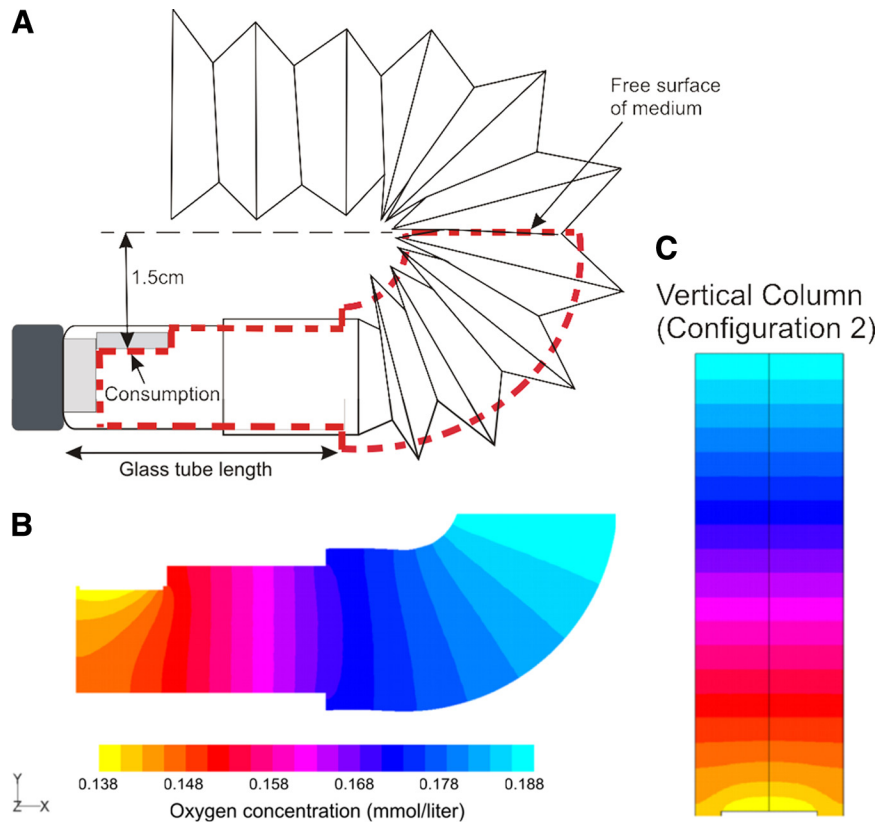


FIGURE 4. Computed oxygen tensions and shear stresses, τ , in the pump system (configurations 1B and 4). (a) The configuration of the culture flask showing selected positioning of the inlet and the outlet tubes, with the coverslip located directly underneath the inlet. (b) Contour plot of shear stress (en face view) on the coverslip in the configuration shown in (a). With an inlet speed of 0.07 m/s, the maximum shear stress on the coverslip in this design reached the threshold value of 10^{-3} Pa. (c) Contours of oxygen concentration on the cross-section of the culture flask in (a). Oxygen carried down toward the cells by oxygenated culture medium is clearly visible as a blue jet extending from the inlet, where it is consumed by the cells. Note the different contour scales compared with Figures 3 and 5.

FIGURE 5. Configuration and contours of computed oxygen tension on the cross-section (symmetry plane) of the horizontal column (configuration 3). (a) Horizontal column configuration, with the dotted red line showing the boundary of the simplified simulation region used in numerical modeling of steady oxygen transport. Note that the corrugations of the corrugated part of the tube were not taken into account in the simulations. (b) Computed oxygen concentration contours on the cross-section of the horizontal column with the length from the open end of the glass tube to the platform being 66 mm, based on 6000 cells on the coverslip. (c) Computed oxygen concentration contours for configuration 2, for the same conditions as shown in (b).



ing a steady state of 50% to 60% of their starting values (Fig. 6). The shape of the curve was different from that predicted theoretically (Fig. 3), being consistent with a slowing of cell

division and/or a downregulation of cellular oxygen consumption rate as oxygen tension decreased. A very similar trend was observed in configuration 4, consistent with oxygen tensions at the inlet of the supply tubing being slowly reduced until reaching a new steady state. Because the supply tubing inlet was placed approximately 1 cm below the free surface of the upper reservoir, oxygen tensions at the inlet will be determined by a balance of diffusion from the free surface of the upper reservoir and mixing of oxygen-depleted medium returned from the culture chamber. Finally, unlike the situation in configurations 1A and 4, oxygen tensions in configuration 2 showed a much more marked decrease, to a value of approximately 10% of the starting tension by 72 hours. This oxygen tension in configuration 2 at 72 hours was only approximately one-fourth of that present in configuration 4 and one-fifth of that present in configuration 1A.

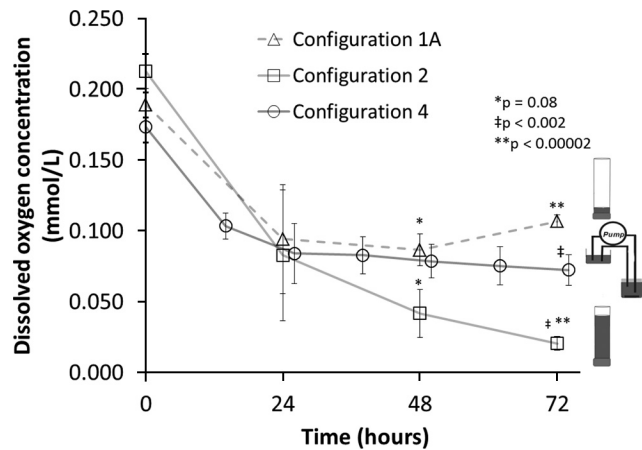


FIGURE 6. Measured oxygen concentrations in three different experimental configurations: control column (configuration 1A); high-pressure column (configuration 2); and high-pressure pump (configuration 4). Points for configuration 4 have been offset by 2 hours on the time axis so as not to overlap points for the other configurations and hence improve the clarity of plotting; in reality they were measured every 12 hours starting at time 0. There was a slight increase in oxygen concentrations at 72 hours in configuration 1A, but this was not significantly different from the value at 48 hours ($P = 0.13$), although it was different from the value in configuration 4 at 72 hours ($P = 0.014$). This increase could be due to experimental error, or to a reduced cellular oxygen consumption rate in conjunction with oxygen diffusion from the free surface. Error bars are SEM at each time point; P values refer to comparison between matching symbols by two-sided t -test at the indicated times.

Experimental Measurements of Cell Migration

After the cell-free area was created, cells migrated into this region, reducing the CFA size with time (Fig. 7). As seen in Figure 8a, under control conditions, there was no significant difference in the cell migration (i.e., in the reduction of the CFA), at any time point between the vertical column (configuration 1A) and the pump system (configuration 1B). This confirms that the pump system itself did not significantly affect the migration of the cells.

Cell migration was significantly faster in vertical columns (configuration 2, low oxygen tension) than in the pump system with the same pressure (configuration 1B, normal oxygen tension) at 48 and 72 hours (Fig. 8b). Similarly, under normal pressure, the migration rate of cells in the horizontal tubes (configuration 3) was faster than in configuration 1A at 48 and 72 hours. This suggests that, under both high pressure and normal pressure conditions, oxygen tension had a significant effect on cell migration, with reduced tension increasing cell migration. This suggests

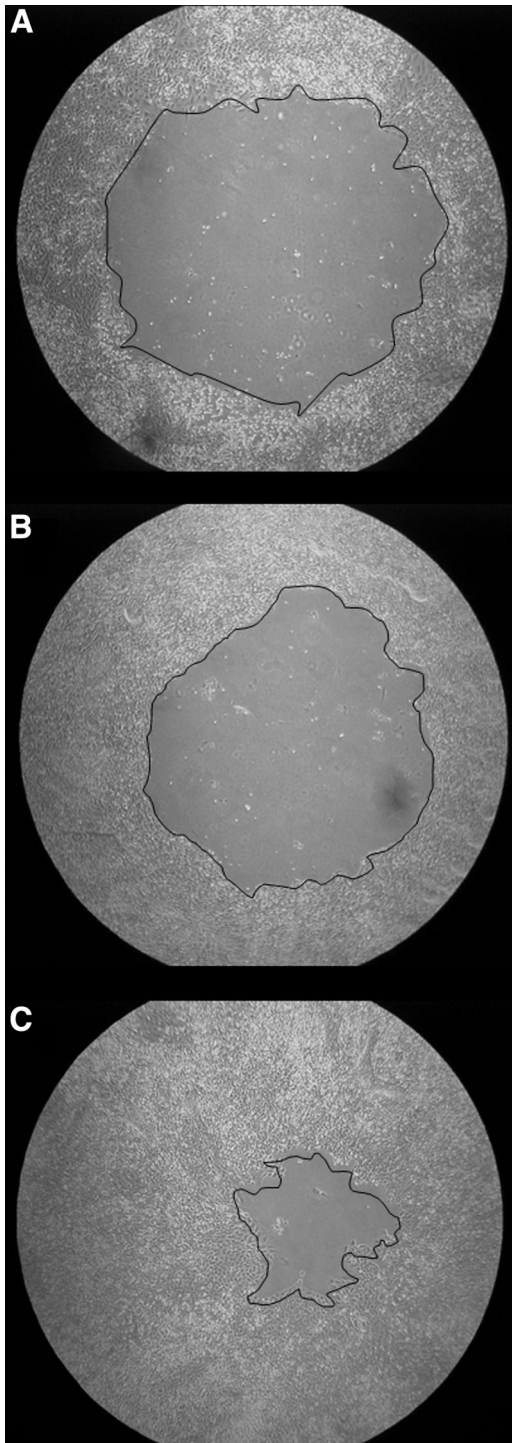


FIGURE 7. Micrographs of DITNC1 cell migration into the cell free area. (a–c) Images taken of three different coverslips after leaving the cells under vertical control pressure (configuration 1) conditions and allowing the cells to migrate into the CFA for 24, 48, and 72 hours, respectively. The edge of the CFA has been traced on each image in *black*; the number of pixels enclosed in the *black curve* was used to calculate the CFA.

that it is not pressure per se that affects cell migration, but rather gas tension in the culture medium.

This is consistent with Figure 8c, which shows the same data plotted in a different manner (i.e., grouped by oxygen tension rather than by pressure). For a given gas tension level, elevated hydrostatic pressure did not significantly increase cell

migration at any time point tested compared with control pressure conditions.

Experimental Measurements of α -Tubulin Staining

We did not observe marked changes of cell morphology or α -tubulin architecture in cells at any time point for any of the experimental conditions (i.e., the shape of α -tubulin architecture was similar under all the conditions; Fig. 9).

DISCUSSION AND CONCLUSIONS

Our goal was to design and use equipment to separately test the effects of pressure and altered gas tension on cultured cells. Our major experimental finding is that pressure alone, at least at the modest levels used in this study (7.4 mm Hg above atmospheric pressure), had no effect on the migration rate or α -tubulin architecture of cultured DITNC1 astrocytes, whereas reduction in oxygen tension was associated with increased cell migration. Hence, it was not hydrostatic pressure, per se, that affected cellular behavior, but rather changes in the dissolved gas concentration in the medium. Our conclusions are broadly similar to those recently reported by Russ et al.,²⁶ who also designed equipment to independently evaluate the effects of pressure and hypoxia on cultured proximal tubule epithelial cells and observed no direct effect of ~ 60 mm Hg pressure. Our conclusions also agree with the results of Obazawa et al.,¹⁵ who measured optineurin and myocilin expression in trabecular meshwork cells after exposure to an elevated pressure of 33 mm Hg for various times, which did not result in any observed changes between control and pressurized cultures. In this context, it is important to consider that when a cell is cultured on a rigid substrate, the elevation of hydrostatic pressure should not lead to any significant cellular deformation; instead, the pressure in the cell should simply rise to match the externally imposed pressure, since the cell membrane is flexible, and the cell is filled with a nearly incompressible fluid (water). Further, theoretical estimates predict that a 50-mm Hg increase in the hydrostatic pressure in a rigid container would lead to relative deformations of cellular components of less than 0.005%.²⁷ It is hard to understand how such minute deformations would lead to biological effects. It is only when cells are grown on a flexible substrate that is deformed by pressure that they experience significant mechanical stimulation (namely, stretch) secondary to elevated pressure.

Our results differ from several reports showing an effect of modest pressure on cell behavior, most notably those of Salvador-Silva et al.,⁴ who used a pressurization system essentially identical with the vertical columns (configurations 1A and 2) used in this study and showed a CFA in their configuration 2 that was approximately 55% smaller than the CFA in their configuration 1A at 72 hours, which was interpreted as a pressure effect. We saw no statistically significant effect of pressure on CFA at 72 hours. There are several possible reasons for this discrepancy. The first is a difference in cell lines; Salvador-Silva et al.⁴ used primary cultures of human astrocytes, whereas we used an immortalized DITNC1 rat astrocyte cell line. In view of the discussion below, we do not believe that this is the most likely explanation; nonetheless, future work should repeat the studies reported here using human astrocytes. The second possible reason is that the effects reported by Salvador-Silva et al.⁴ were due to alterations of gas tension in the culture medium, secondary to experimental conditions intended to change only hydrostatic pressure. Changes in gas tension affect cell function by changing the concentration of dissolved oxygen and carbon dioxide in the medium, influencing cellular metabolism and affecting local pH. Based on our direct measurements of oxygen tension and

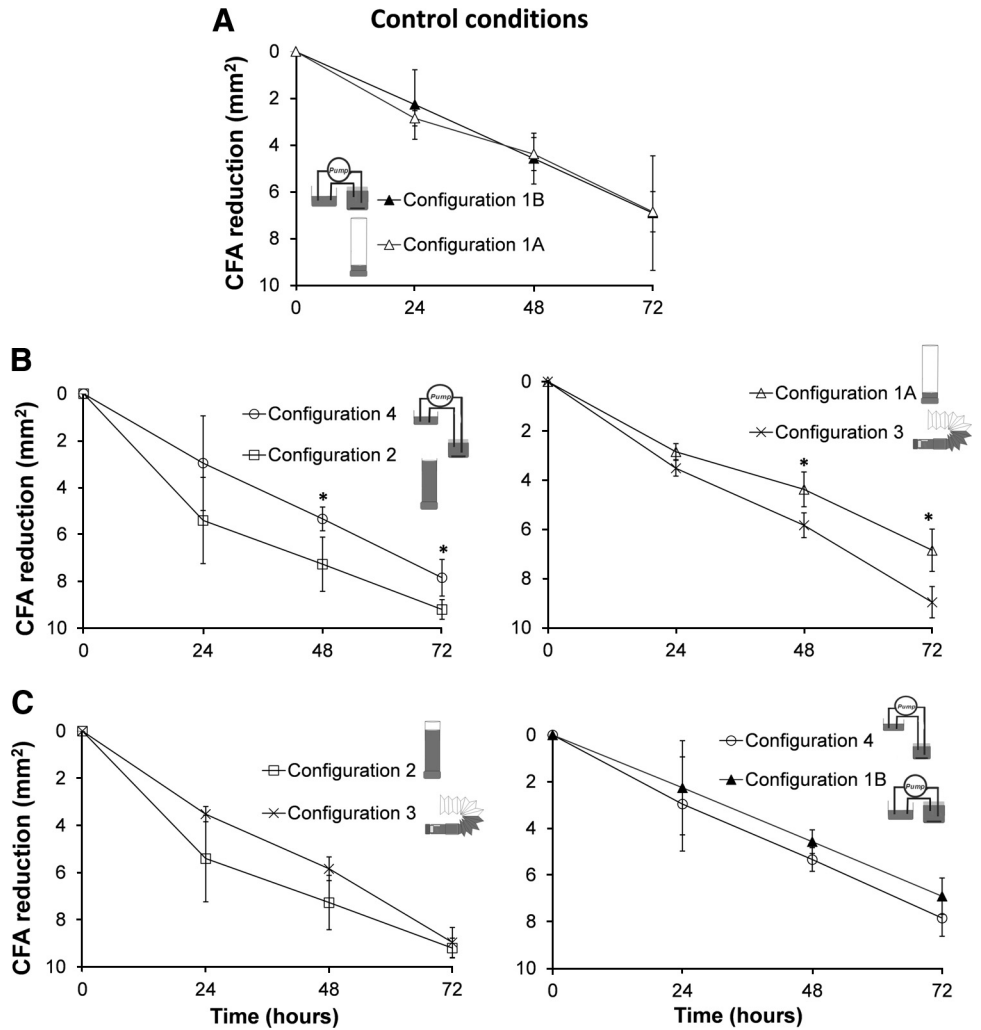


FIGURE 8. Comparisons of cell migration under different experimental conditions. The vertical axis in all graphs is the area of the cell-free area that has been repopulated by cells after the creation of the cell-free area at time 0. (a) There is no significant difference in cell migration into the CFA under control conditions (normal pressure and normal oxygen tension) between the pump (configuration 1B) and vertical column (configuration 1A). (b) Low oxygen tension significantly increased cell migration at 48 hours and 72 hours; **P* < 0.05. (c) High hydrostatic pressure did not significantly increase cell migration. Note that the nominal starting CFA was ~12.4 mm², but because of occasional cell ingrowth under the disc or removal of some cells adhering to the disc, the starting CFA varied from one experiment to the next; therefore all data are expressed in terms of the reduction of the CFA.

the physical arguments presented below, we believe that the latter explanation is much more likely.

Alteration in the gas tension within the cell culture medium can occur in a variety of ways, depending on the experimental conditions and precisely how the hydrostatic pressure is applied. In fact, it is quite difficult to change hydrostatic pressure without also affecting gas tension in the culture medium, unless a pump (e.g., configurations 1B and 4) or similar arrangement is used. In the following discussion, we describe two of the most commonly used experimental designs to apply hydrostatic pressure, and we discuss how these designs inadvertently lead to changes in the dissolved gas concentration.

In the first approach, a column of medium is applied over the cultured cells (i.e., they are cultured at the bottom of a tube partially filled with medium), and the height of the medium column is varied to control the hydrostatic pressure acting on the cells.^{4,10,28,29} The overlying medium increases the diffusion distance between the cells and the gas-liquid interface, thereby presenting a greater barrier to transporting oxygen to the cells once oxygen in the medium is depleted. This occurs for times greater than the diffusion equilibration timescale $L^2/(4D)$, which is approximately 5 hours for standard culture conditions. Our results and the discussion below indicate that this can lead to hypoxia under some conditions.

In the second approach, the gas pressure surrounding the culture medium is increased, typically by enclosing the culture dishes in a chamber connected to a pressurized gas source.^{2,3,5-8,11-13,30-33} Henry's law shows that changing

the composition and/or pressure of the gas in contact with the culture medium will change the gas tensions and pH in the medium and hence will potentially indirectly influence cellular physiology. More specifically, changes in soluble O₂ and CO₂ are unavoidable when using compressed air and can be avoided only if the compressed gas is carefully chosen to maintain the same standard partial pressures of metabolic gas species (e.g., O₂ and CO₂) while making up the remaining partial pressure with an inert gas (e.g., N₂).

In light of these potentially complex effects, it would be valuable, when studying pressure effects on cultured cells, to include robust controls along the lines of those we have used here or those reported by Russ et al.²⁶ More specifically, we recommend that future studies should include an in-dwelling oxygen sensor so that oxygen tensions at the level of the cells can be directly measured. We particularly emphasize that an in-dwelling sensor is preferable to approaches where samples of media are withdrawn and analyzed, since this technique likely creates unrealistic mixing (during sampling) and equilibration of gases in the sample with the atmosphere (while the sample is being prepared for analysis).

Design of Experimental Apparatus and Oxygen Tensions

The pump recirculation method proposed by Obazawa et al.¹⁵ and refined here turned out to be an excellent way to pressurize cells without altering the gas tension in the medium. By

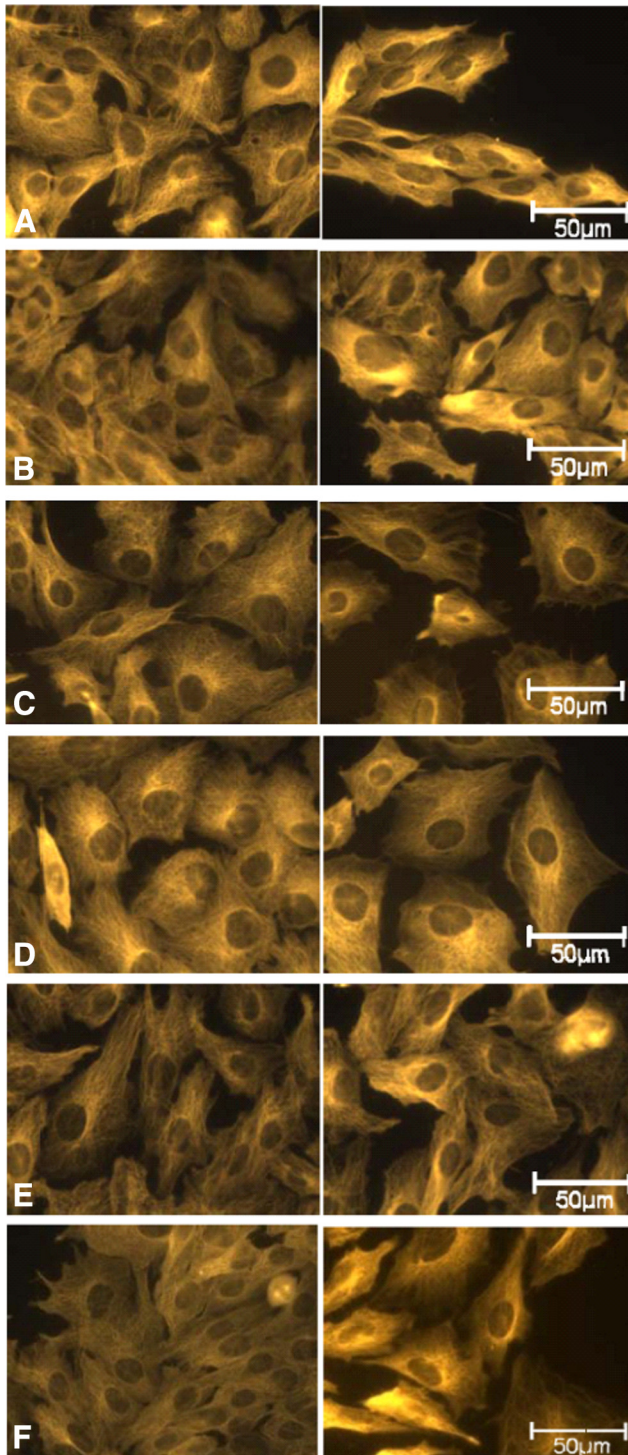


FIGURE 9. α -Tubulin staining of DITNC1 cells cultured under five different configurations: (a) horizontal columns (configuration 3), (b) vertical column under control pressure (configuration 1A), (c) vertical column under high hydrostatic pressure (configuration 2), (d) pump system under control pressure (configuration 1B), (e) pump system under high hydrostatic pressure (configuration 4), (f) untreated cells left in Petri dishes. The images were taken from cells close to the edge of the CFA. Each set of two images in a row are from the same condition and were obtained from two independent coverslips exposed to the relevant condition for 48 hours.

choosing culture chamber dimensions, the positions of inlet and outlet tubes and the medium flow rate, our design exposed cells to adequate oxygenation but minimal shear stress. The

hydrostatic pressure applied to the cells in this configuration can easily be increased by elevating the medium reservoir, while maintaining gas tensions in the culture medium at a level comparable to that expected in a standard culture dish (Fig. 6).

The situation with gas tensions in the medium is more complex in the case of static fluid columns. Here, we discuss oxygen tensions, since they are likely the most physiologically relevant; similar comments apply to other gas species. Oxygen tensions will depend on the duration of the experiment, the initial amount of dissolved oxygen in the medium (which our results show may differ between individual medium bottles and is not usually equal to the value expected for medium in equilibrium with air), cellular consumption rates, and the amount of mixing that the medium undergoes. Mixing can be active—for example, via medium changes or shaking of the culture chambers (e.g., incubator vibration)—or passive, through free convection. We estimated whether free convection would occur or not (due to density differences driven by the cells' metabolic activities) and concluded that it was unlikely to occur.¹⁷ Thus, modeling work considered oxygen transport through a stagnant fluid column.

This modeling suggests that the cells in short columns (configuration 1A) have a greater capacity to delay or minimize hypoxia than cells in tall columns (configuration 2) (e.g., by reducing cellular growth rate; Fig. 3). The different responses between tall and short columns is attributable to differences in the physics of oxygen transport for configurations 1A and 2, as expressed by equations 6 and 7. For large γt , but before the oxygen deficit starts to interact with the free surface in configuration 2, both equations can be written in the form

$$c(z = 0, t) = \text{const} - \Lambda \frac{n_o \beta e^{\gamma t}}{\pi r^2 D} \quad (8)$$

where the constant Λ equals the column depth L for configuration 1A and equals $\sqrt{D/\gamma}$ for configuration 2. Accordingly, a decrease in γ is less effective in reducing hypoxia in configuration 2 than in configuration 1A, because in configuration 2 the decrease in the $e^{\gamma t}$ term is opposed by the increase in Λ as γ is reduced. Configuration 2 is thus more limited in its ability to provide oxygen to cells. For example, if cells reduce their metabolic rate by a factor of two, Figure 3 predicts that after 72 hours (the longest interval between medium change in our experiments), cells will experience oxygen tensions about half of ambient in configuration 1A, but approximately 16-fold less than ambient in configuration 2.

These predicted behaviors are broadly consistent with our direct oxygen measurements, where it is clear that oxygen tensions in configuration 2 were less than those in configurations 1A and 4, for times greater than 48 hours (Fig. 6). We note parenthetically that these measurements, which show an approach to steady oxygen concentration for large times, differ from the behavior shown in Figure 3. This strongly suggests that cell division and/or oxygen consumption rate were reduced in our experiments as oxygen tension decreased and points out a shortcoming in the theoretical calculations—namely, the assumption of constant cell division and oxygen consumption rates. Nonetheless, the theoretical calculations are useful in understanding the basic physics involved. In any case, it is clear that the static fluid column (configuration 2) represents a significant barrier to oxygen transport and that cells grown under this configuration experience appreciably reduced oxygen tensions. It is noteworthy that even in the “standard” arrangement (configuration 1A), cells do not necessarily experience the oxygen tensions present in the incubator atmosphere. Rather, the initial oxygen (or CO_2) tension is determined by the dissolved oxygen (or CO_2) concentration in the newly opened bottle of medium, which varies from one bottle

to the next, unless each medium is carefully pre-equilibrated with standard incubator gasses. This often-overlooked bottle-to-bottle variability could be a source of error in cell culture experiments.

Summary

We found no effect of modest pressure (7.4 mm Hg) on cultured astrocyte migration rates and α -tubulin architecture. This suggests that previous results obtained with a similar system were an artifact of gas transport rather than pressure per se. Future studies examining the effects of modest hydrostatic pressure on cells should include a broader range of controls. It would also be interesting to study additional outcome measures beyond those reported here.

Finally, we suggest that more attention be paid to the details of applied pressure magnitudes when quoting previous studies. For example, one oft-quoted study saw effects after cells were exposed to 5 MPa of pressure,³⁴ which is approximately 37,500 mm Hg. Although suitable for studying mechanobiologic effects in cartilage, for example, this is clearly much higher than expected in glaucoma. The results of such studies need to be put in context (i.e., effects observed at 5 MPa would seem to establish little precedent for a direct effect of more modest pressures [<100 mm Hg] on cells).

References

- Goldberg I. Relationship between intraocular pressure and preservation of visual field in glaucoma. *Surv Ophthalmol.* 2003;48: S3-S7.
- Wax MB, Tezel G, Kobayashi S, Hernandez MR. Responses of different cell lines from ocular tissues to elevated hydrostatic pressure. *Br J Ophthalmol.* 2000;84:423-428.
- Agar A, Li S, Agarwal N, Coroneo MT, Hill MA. Retinal ganglion cell line apoptosis induced by hydrostatic pressure. *Brain Res.* 2006; 1086:191-200.
- Salvador-Silva M, Aoi S, Parker A, Yang P, Pecan P, Hernandez MR. Responses and signaling pathways in human optic nerve head astrocytes exposed to hydrostatic pressure in vitro. *Glia.* 2004;45: 364.
- Agar A, Yip SS, Hill MA, Coroneo MT. Pressure related apoptosis in neuronal cell lines. *J Neurosci Res.* 2000;60:495-503.
- Liu Q, Ju WK, Crowston JG, et al. Oxidative stress is an early event in hydrostatic pressure induced retinal ganglion cell damage. *Invest Ophthalmol Vis Sci.* 2007;48:4580-4589.
- Tezel G, Wax MB. Increased production of tumor necrosis factor- α by glial cells exposed to simulated ischemia or elevated hydrostatic pressure induces apoptosis in cocultured retinal ganglion cells. *J Neurosci.* 2000;20:8693-8700.
- Ju WK, Liu Q, Kim KY, et al. Elevated hydrostatic pressure triggers mitochondrial fission and decreases cellular ATP in differentiated RGC-5 cells. *Invest Ophthalmol Vis Sci.* 2007;48:2145-2151.
- Burgoyne CF, Quigley HA, Thompson HW, Vitale S, Varma R. Early changes in optic disc compliance and surface position in experimental glaucoma. *Ophthalmology.* 1995;102:1800.
- Hernandez MR, Pena JD, Selvidge JA, Salvador-Silva M, Yang P. Hydrostatic pressure stimulates synthesis of elastin in cultured optic nerve head astrocytes. *Glia.* 2000;32:122.
- Ricard CS, Kobayashi S, Pena JD, Salvador-Silva M, Agapova O, Hernandez MR. Selective expression of neural cell adhesion molecule (NCAM)-180 in optic nerve head astrocytes exposed to elevated hydrostatic pressure in vitro. *Brain Res Mol Brain Res.* 2000;81:62-79.
- Liu B, Neufeld AH. Nitric oxide synthase-2 in human optic nerve head astrocytes induced by elevated pressure in vitro. *Arch Ophthalmol.* 2001;119:240-245.
- Yang JL, Neufeld AH, Zorn MB, Hernandez MR. Collagen type I mRNA levels in cultured human lamina cribrosa cells: effects of elevated hydrostatic pressure. *Exp Eye Res.* 1993;56:567-574.
- Yang P, Agapova O, Parker A, et al. DNA microarray analysis of gene expression in human optic nerve head astrocytes in response to hydrostatic pressure. *Physiol Genomics.* 2004;17:157.
- Obazawa M, Mashima Y, Sanuki N, et al. Analysis of porcine optineurin and myocilin expression in trabecular meshwork cells and astrocytes from optic nerve head. *Invest Ophthalmol Vis Sci.* 2004;45:2652-2659.
- Cussler EL. *Diffusion: Mass Transfer in Fluid Systems.* New York: Cambridge University Press; 1997.
- Rajabi S. *Response of Astrocytes Exposed to Elevated Hydrostatic Pressure and Hypoxia.* Master's thesis. Toronto: Department of Mechanical and Industrial Engineering, The Institute of Biomaterials and Biomedical Engineering, University of Toronto; 2008.
- Rouleau C, Rakotoarivelo C, Petite D, et al. Pyruvate modifies glycolytic and oxidative metabolism of rat embryonic spinal cord astrocyte cell lines and prevents their spontaneous transformation. *J Neurochem.* 2007;100:1589-1598.
- Jacobson J, Duchon MR, Hothersall J, Clark JB, Heales SJ. Induction of mitochondrial oxidative stress in astrocytes by nitric oxide precedes disruption of energy metabolism. *J Neurochem.* 2005; 95:388-395.
- Hasselblatt M, Bunte M, Dringen R, et al. Effect of endothelin-1 on astrocytic protein content. *Glia.* 2003;42:390-397.
- Chaudhry MA, Zubair SM. Heat conduction in a semi-infinite solid subject to time-dependent surface heat fluxes: an analytical study. *Warme Und Stoffubertragung.* 1993;28:357-364.
- Janmey PA, McCulloch CA. Cell mechanics: integrating cell responses to mechanical stimuli. *Annu Rev Biomed Eng.* 2007;9:1-34.
- Orr AW, Helmke BP, Blackman BR, Schwartz MA. Mechanisms of mechanotransduction. *Dev Cell.* 2006;10:11-20.
- Guo P, Weinstein AM, Weinbaum S. A hydrodynamic mechanosensory hypothesis for brush border microvilli. *Am J Physiol.* 2000;279:F698-F712.
- Radany EH, Brenner M, Besnard F, Bigornia V, Bishop JM, Descheppe CF. Directed establishment of rat brain cell lines with the phenotypic characteristics of type 1 astrocytes. *Proc Natl Acad Sci U S A.* 1992;89:6467-6471.
- Russ AL, Dadarlat IA, Haberstroh KM, Rundell AE. Investigating the role of ischemia vs. elevated hydrostatic pressure associated with acute obstructive uropathy. *Ann Biomed Eng.* 2009;37:1415-1424.
- Ethier CR, Johnson M. Hydrostatic pressure is not a surrogate for IOP in glaucoma (E-Letter). *Invest Ophthalmol Vis Sci.* 2006.
- Liu B, Neufeld AH. Activation of epidermal growth factor receptor signals induction of nitric oxide synthase-2 in human optic nerve head astrocytes in glaucomatous optic neuropathy. *Neurobiol Dis.* 2003;13:109.
- Neufeld AH, Liu B. Comparison of the signal transduction pathways for the induction of gene expression of nitric oxide synthase-2 in response to two different stimuli. *Nitric Oxide.* 2003;8:95-102.
- Sappington RM, Calkins DJ. Contribution of TRPV1 to microglia-derived IL-6 and NF κ B translocation with elevated hydrostatic pressure. *Invest Ophthalmol Vis Sci.* 2008;49:3004-3017.
- Sappington RM, Calkins DJ. Pressure-induced regulation of IL-6 in retinal glial cells: involvement of the ubiquitin/proteasome pathway and NF κ B. *Invest Ophthalmol Vis Sci.* 2006;47:3860-3869.
- Sappington RM, Chan M, Calkins DJ. Interleukin-6 protects retinal ganglion cells from pressure-induced death. *Invest Ophthalmol Vis Sci.* 2006;47:2932-2942.
- Sappington RM, Sidorova T, Long DJ, Calkins DJ. TRPV1: contribution to retinal ganglion cell apoptosis and increased intracellular Ca²⁺ with exposure to hydrostatic pressure. *Invest Ophthalmol Vis Sci.* 2009;50:717-728.
- Knight MM, Toyoda T, Lee DA, Bader DL. Mechanical compression and hydrostatic pressure induce reversible changes in actin cytoskeletal organization in chondrocytes in agarose. *J Biomechan.* 2006;39:1547-1551.